Journal of the Korean Magnetic Resonance Society **2020**, *24,* 96-103
DOI http://dx.doi.org/10.6564/JKMRS.2020.24.4.096

Solvent-localized *in-situ* NMR Monitoring by Intermolecular Single-quantum Coherence Study

Jin Wook Cha[1,*] and Sunghyouk Park[2]

[1]Natural Product Informatics Research Center, KIST Gangneung Institute of Natural Products, Gangneung 25451, Republic of Korea
[2]Natural Product Research Institute, College of Pharmacy, Seoul National University, 1 Gwanak-ro, Gwanak-gu, Seoul 08826, Republic of Korea

Received December 11, 2020; Revised December 18, 2020; Accepted December 18, 2020

Abstract A new NMR method to monitor solvent-localized NMR signals in the two-phase liquid system is suggested. This method based on intermolecular single-quantum coherence (iSQC). Here, we exploited the feature of the local action of distant dipolar field (DDF) effect in order to filter out specific NMR signals dissolved in different solvents. This solvent specific iSQC spectroscopy was carried out on a model two-phase liquid system (D-glucose in water/palmitic acid in chloroform), and showed solvent-localized NMR signals. We believe our approaches might be useful in metabolic analysis such as two-phase liquid extraction scheme for labile chemical species.

Keywords DDF, iSQC, mixture analysis, two-phase liquid extraction

Introduction

In 1990s, a series of theoretical[1-3] explanation and experimental[4] demonstration of long-range dipolar interaction in liquid NMR were presented by Warren group. Since then, features such as the local action of the DDF effect[5] and associated applicability for the inhomogeneous magnetic field[6] have attracted the attention of many NMR researchers. Several variant of experiments based on DDF effect have been proposed, for example, intermolecular zero-[6], double-[7] and single-[8] quantum coherences. Chen *et al.*[9] proposed 'IDEAL method' which gives high-resolution NMR spectra in the moderate inhomogenous field condition by distant dipolar interactions between the solvent and solute nuclear spins. Faber *et al.* [10] suggested a method, for a separation of intra- and extracellular component signals, which exploits the local action of DDF. Recently, as a study to expand the applicability of DDF effect to biological samples, Fugariu *et al.*[11] reported the applicability of in-vivo metabolomics in DDF-based experiments by employing an adiabatic mixing pulse to the iSQC type experiment.

Two-phase Liquid Extraction (TLE) has been employed in many chemical and biological procedures for the purpose of separation or purification of chemical species according to their solubility and polarity. For the most cases, the analysis of TLE component by spectroscopic or spectrometric methods, additional procedures are usullay required. However, in the case of labile or volatile compounds, degradation or loss of compounds during this process is likely to occur. While the solution-state NMR spectroscopy, in principle, can provide structural information through the non-destructive process, it also reflects whole signals included in sample. These features hamper the *in-situ* monitoring of individual phase information within the

* Address correspondence to: **Jin Wook Cha,** Natural Product Informatics Research Center, KIST Gangneung Institute of Natural Products, Gangneung 25451, Republic of Korea, Tel: 82-33-650-3511; E-mail: elmarit@kist.re.kr

two-phase system using the conventional NMR spectroscopic methods.

In light of this, we suggest new method which can distinguish individual NMR signals dissolved in a specific solvent based on iSQC sequence by choosing solvent selective excitation pulses. Here, a brief theoretical description of iSQC study were presented and the feasibility of new method was tested in a model of two-phase liquid system; D-glucose in water/ palmitic acid in chloroform.

Theory of iSQC sequence

iSQC sequence for the acquiring solvent selective solute NMR signals is shown as Figure 1A. We consider equilibrium state consist of single solute spin-**S** included in sovent spin-**I** (**I**+**S** spin system). At the initial equilibrium state, the reduced density operators are

$$\begin{aligned}\hat{\sigma}^{eq}{}_{\mathrm{I}} &= \hat{I}_z \\ \hat{\sigma}^{eq}{}_{\mathrm{S}} &= \hat{S}_z\end{aligned} \tag{1}$$

where $\hat{I}_z$ is the solvent polarization which is large amount than a solute spin and $\hat{S}_z$ is the solute polarization which is small amount compare to solvent spin. For brevity, we neglected radiation damping, diffusion and relaxation during the entire pulse sequence and effect of adiabatic spinlock (consider as a simple spin-echo) and WATERGATE sequence. In iSQC sequence, the first selective $(\pi/2)_x^I$-pulse gives rise to transeverse polarization $-\hat{I}_y$. During the t_1-evolution period, **I**-spin further evolved by Zeeman interaction, z-gradient pulse and unknown field inhomogeneity, $\Delta B(z)$.

$$\begin{aligned}&\hat{S}_z + \hat{I}_z \xrightarrow{(\pi/2)_x^I} \hat{S}_z - \hat{I}_y \xrightarrow{\gamma Gz\delta} \xrightarrow{\Omega_I \hat{I}_z t_1} \\ &\hat{S}_z - \hat{I}_y \cos(\gamma Gz\delta + \Omega_I t_1 + \gamma\Delta B(z)t_1) \\ &\quad + \hat{I}_x \sin(\gamma Gz\delta + \Omega_I t_1 + \gamma\Delta B(z)t_1)\end{aligned} \tag{2}$$

where, $\boldsymbol{\gamma}$ is the gyromagnetic ratio of nucleus, $\boldsymbol{Gz}$ is the field gradient according to z-axis position of spins, $\boldsymbol{\delta}$ is the duration of gradient pulse and $\boldsymbol{\Omega_I \hat{I}_z}$ ($\boldsymbol{\Omega_I}$ is the frequency offset of **I**-spin) is the hamiltonian of Zeeman interaction of the **I**-spin.

After selective rotation about x-axis of **S**-spin, then both of **I**- and **S**-spin evolved together by the z-gradient pulse. Before the adiabatic spinlock delay, thus, each spin density operator has a form of

$$\begin{aligned}&\hat{S}_z - \hat{I}_y \cos(\gamma Gz\delta + \Omega_I t_1 + \gamma\Delta B(z)t_1) \\ &+ \hat{I}_x \sin(\gamma Gz\delta + \Omega_I t_1 + \gamma\Delta B(z)t_1) \\ &\qquad \xrightarrow{(\pi/2)_x^{I+S}} \xrightarrow{(-\pi/2)_x^I} \xrightarrow{\gamma 0.7 Gz\delta} \\ &-\hat{S}_y \cos(0.7\gamma Gz\delta) + \hat{S}_x \sin(0.7\gamma Gz\delta) \\ &- \hat{I}_y \cos(1.7\gamma Gz\delta + \Omega_I t_1 + \gamma\Delta B(z)t_1) \\ &+ \hat{I}_x \sin(1.7\gamma Gz\delta + \Omega_I t_1 + \gamma\Delta B(z)t_1)\end{aligned} \tag{3}$$

After applyting of series of non-selective inversion pulse, π_x^{I+S}, **I**-spin selective pulse, $(\pi/2)_x^I$, and z-gradient pulse the density operators can be expressed as

$$\begin{aligned}&-\hat{S}_y \cos(0.7\gamma Gz\delta) + \hat{S}_x \sin(0.7\gamma Gz\delta) \\ &- \hat{I}_y \cos(1.7\gamma Gz\delta + \Omega_I t_1 + \gamma\Delta B(z)t_1) \\ &+ \hat{I}_x \sin(1.7\gamma Gz\delta + \Omega_I t_1 + \gamma\Delta B(z)t_1) \\ &\qquad \xrightarrow{\pi_x^{I+S}} \xrightarrow{(\pi/2)_x^I} \xrightarrow{\gamma 2.4 Gz\delta} \\ &\hat{S}_y \cos(-1.7\gamma Gz\delta) + \hat{S}_x \sin(-1.7\gamma Gz\delta) \\ &+ \hat{I}_z \cos(1.7\gamma Gz\delta + \Omega_I t_1 + \gamma\Delta B(z)t_1) \\ &+ \frac{1}{2}\hat{I}_x\{\sin(4.1\gamma Gz\delta + \Omega_I t_1 + \gamma\Delta B(z)t_1) \\ &+ \sin(-0.7\gamma Gz\delta + \Omega_I t_1 + \gamma\Delta B(z)t_1)\} \\ &+ \frac{1}{2}\hat{I}_y\{\cos(4.1\gamma Gz\delta + \Omega_I t_1 + \gamma\Delta B(z)t_1) \\ &- \cos(-0.7\gamma Gz\delta + \Omega_I t_1 + \gamma\Delta B(z)t_1)\}\end{aligned} \tag{4}$$

Then, from the equation **(4),** we can separate the spin-density operator into each of spin-specific terms, respectively, as follows

$$\begin{aligned}\hat{\sigma}_{\mathrm{I}}(t_1, z) = &\\ &\hat{I}_z \cos(\Omega_I t_1 + 1.7\gamma Gz\delta + \gamma\Delta B(z)t_1) \\ &+ \Big[\frac{1}{2}\hat{I}_x\{\sin(4.1\gamma Gz\delta + \Omega_I t_1 + \gamma\Delta B(z)t_1) \\ &+ \sin(-0.7\gamma Gz\delta + \Omega_I t_1 + \gamma\Delta B(z)t_1)\} \\ &+ \frac{1}{2}\hat{I}_y\{\cos(4.1\gamma Gz\delta + \Omega_I t_1 + \gamma\Delta B(z)t_1) \\ &- \cos(-0.7\gamma Gz\delta + \Omega_I t_1 + \gamma\Delta B(z)t_1)\}\Big] \\ \hat{\sigma}_{\mathrm{S}}(t_1, z) = \hat{S}_x \sin(-1.7\gamma Gz\delta) + \hat{S}_y \cos(-1.7\gamma Gz\delta)&\end{aligned} \tag{5}$$

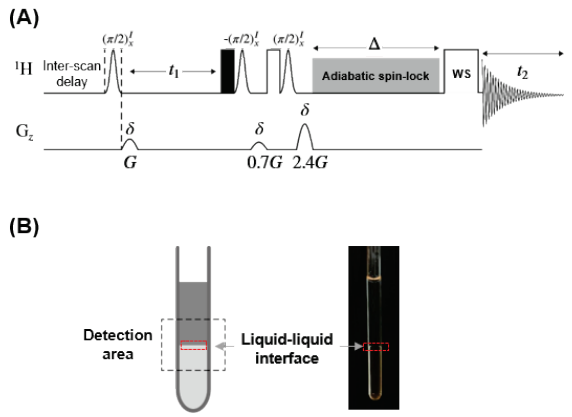

Figure 1. (A) Pulse sequence for solvent-localized NMR spectra using iSQC sequence. A black bar is non-selective excitation pulse and a white bar is non-selective inversion pulse. A gray box is adiabatic spinlock pulse sequence and a white box including 'WS' is "W5" binomial pulse sequence with double gradient echo for the solvent suppression. Gauss shaped pulses are selective excitation pulses, semi-ellipsoidal pulses are *z*-gradient pulses. All pulses are of phase, *x* unless otherwise indicated.; *See experimental section for details*. **(B)** Pictorial illustration (right) and real picture (left) of a two-phase liquid NMR sample. Dashed-box indicates NMR detection area in NMR tube. Solid box indicates an interface between two immiscible liquid phases.

Since, after this, there is no more pulses which can result in a coherence transfer for the $\hat{I}_{xy}$-spin, we will omit $\hat{I}_{xy}$ product operator term in rest of the pulse sequence. According to distant dipolar field (DDF) theory[12], a spatially modulated *z*-magnetization is the source of DDF along the *z*-direction.

$$B_D^S(z) = -\frac{2}{3\tau_{dI}}\cos(\Omega_I t_1 + 1.7\gamma G z\delta + \gamma\Delta B(z)t_1) \qquad \textbf{(6)}$$

where, B_D^S is the dipolar field experienced by **S**-pin and $\tau_{dI} = (\gamma\mu_0 M_0^I)^{-1}$; μ_0 is the vacuum magnetic permeability and M_0^I is the equilibrium magnetization per unit volume of **I**-spin.

From the modified Bloch equation,

$$\frac{d\mathbf{M}_{xy}}{dt} = -i\gamma\left(\mathbf{M}_{xy}\boldsymbol{B}_z - \boldsymbol{B}_{xy}\mathbf{M}_z\right) - \frac{\mathbf{M}_{xy}}{T_2} \qquad \textbf{(7)}$$

we can evaluate observable operators during the acquisition period, t_2, including Zeeman ($\Omega_S\hat{I}_z$) and dipolar interaction (by DDF), as follows,

$$\begin{aligned}&\hat{\sigma}_S(t_1, t_2', z)\\ &= \hat{S}_x\sin\{-1.7\gamma G z\delta - \Omega_S t_2 - \gamma\Delta B(z)t_2 - B_D^S(z)t_2'\}\\ &+ \hat{S}_y\cos\{-1.7\gamma G z\delta - \Omega_S t_2 - \gamma\Delta B(z)t_2 - B_D^S(z)t_2'\}\end{aligned} \qquad \textbf{(8)}$$

Since the only observable operator is $\hat{S}_-$

$$\begin{aligned}&\hat{\sigma}_S(t_1, t_2', z)\\ &= \hat{S}_-\frac{i}{2}\cdot\exp(i1.7\gamma G z\delta)\exp\{i\gamma\Omega_S t_2 + i\gamma B_D^S(z)t_2'\}\\ &\hat{\sigma}_S(t_1, t_2', z)\\ &= \frac{i}{2}\hat{S}_-\exp\left[i\left\{1.7\gamma G z\delta + \Omega_S t_2 + \gamma\Delta B(z)t_2\right.\right.\\ &\left.\left.+\frac{2}{3}\tau_{dI}\cos(\Omega_I t_1 + 1.7\gamma G z\delta + \gamma\Delta B(z)t_1)\,t_2'\right\}\right]\end{aligned} \qquad \textbf{(9)}$$

where, $t_2' = t_2 + \Delta$

Using the Jacobi-Anger expansion,

$$\exp(iz\cos\theta) \equiv \sum_{m=-\infty}^{\infty} i^m J_m(z)\exp(im\theta) \qquad \textbf{(10)}$$

where, $J_m(z)$ is the first-kind Bessel function.

the signal has a form of

$$\begin{aligned}&\hat{\sigma}_S(t_1, t_2', z)\\ &= \frac{i}{2}\hat{S}_-\exp(i\Omega_S t_2)\exp(i1.7\gamma G z\delta)\exp(i\gamma\Delta B(z)t_2)\\ &\times\sum_{m=-\infty}^{\infty} i^m J_m\left(\frac{2}{3}\tau_{dI}^{-1}t_2'\right)\\ &\times\exp(im\Omega_I t_1 + m1.7\gamma G z\delta + m\gamma\Delta B(z)t_1)\end{aligned} \qquad \textbf{(11)}$$

Because the total magnetization in a detection area is the integration of every magnetization along the *z*-axis, we can evaluate the intensity of observable signals by simply adding up the acquired phase, $\sum_{m=-\infty}^{\infty}\exp(i\gamma 1.7(m+1)Gz\delta)$, in along the *z*-axis in a detection range, *L*.

$$\begin{aligned}S_{\text{avg,real}} &= \frac{1}{L}\int_{-\frac{1}{2}L}^{+\frac{1}{2}L}\sum_{m=-\infty}^{\infty}\exp(i\gamma 1.7(m+1)Gz\delta)\,dz\\ &\times(z\text{-gradient independent terms} = \text{A})\\ &= \text{A}\sum_{m=-\infty}^{\infty}\frac{\sin\left(L\frac{1}{2}1.7(m+1)\gamma G\delta\right)}{L\frac{1}{2}1.7(m+1)\gamma G\delta}\\ &= \text{A}\sum_{m=-\infty}^{\infty}\frac{\sin x}{x};\ \text{where} = L\frac{1}{2}1.7(m+1)\gamma G\delta\\ &= \text{A}\sum_{m=-\infty}^{\infty}\text{sinc}(x)\end{aligned} \qquad \textbf{(12)}$$

$S_{\text{avg,real}}$ has a form of the *sinc* function decayed over the length *L*.

A typical length of the detection ranges of the NMR tube along the z-axis is amount to 1 to 2 centimeters, thereby, a spatial averaging will vanish all the signal terms except for m = -1 term which is independent of the spatial position. Thus, the observable signals (m=-1; z-independent terms) can be expressed as,

$$\begin{aligned}
&\hat{\sigma}_S(t_1, t_2', z) \\
&= +\frac{1}{2}\hat{S}_- \exp(i\Omega_S t_2)\exp(-i\Omega_I t_1)\exp(-i\gamma\Delta B(z)t_1) \\
&\times \exp(i\gamma\Delta B(z)t_2)\, J_{-1}\left(\frac{2}{3}\tau_{dI}^{-1}t_2'\right) \\
&\quad \text{Using the identity, } J_{-m} = (-1)^m J_m(x) \\
&= -\frac{1}{2}\hat{S}_- \exp(i\Omega_S t_2)\exp(-i\Omega_I t_1)\exp(-i\gamma\Delta B(z)t_1) \\
&\times \exp(i\gamma\Delta B(z)t_2)\, J_1\left(\frac{2}{3}\tau_{dI}^{-1}t_2'\right)
\end{aligned} \tag{13}$$

On the other hands, we can get same result based on a quantum mechanical description by the intermolecular dipole-dipole interaction phenomena[1]; *See appendix.*

Since, $\langle M_S^+ \rangle(t_1, t_2', z) = \mathrm{Tr}(M_S^+ \cdot \hat{\sigma}_S)$; $M_S^+ = \gamma\hbar\hat{S}_+$

$$\begin{aligned}
&\langle M_S^+ \rangle(t_1, t_2', z) \\
&= -\gamma\hbar\frac{1}{2}\exp(i\Omega_S t_2)\exp(-i\Omega_I t_1)\exp(-i\gamma\Delta B(z)t_1) \\
&\quad \times \exp(i\gamma\Delta B(z)t_2)\, J_1\left(\frac{2}{3}\tau_{dI}^{-1}t_2'\right)
\end{aligned} \tag{14}$$

If the signal has non-zero field inhomogeneity ($\Delta B(z) \neq 0$), the double Fourier transform of the signal results in a group of peak, tilted at an angle of 45-degree, derived from the z-axis position of each spin. By simple counter-clockwise 45-degree rotation followed by a projection along the F_2 dimension will reconstruct desirable 1D NMR spectrum. If we consider, on the other hands, N-weakly coupled spin system for **S**-spins, then the signal form will be changed due to a scalar coupling interaction during the Δ as follows,

$$\begin{aligned}
&\langle M_{S_k}^+ \rangle(t_1, t_2', z) \\
&= -\gamma\hbar\frac{1}{2}\exp(i\Omega_{S_k} t_2)\exp(-i\Omega_I t_1)\exp(-i\gamma\Delta B(z)t_1) \\
&\quad \times \exp(i\gamma\Delta B(z)t_2)\, J_1\left(\frac{2}{3}\tau_{dI}^{-1}t_2'\right) \\
&\quad \times \prod_{l=1}^{N-1}\cos\{\pi J_{kl}(\Delta + t_2)\}
\end{aligned} \tag{15}$$

where, J_{kl} is the intramolecular J-coupling constant between $\hat{S}_k$ and $\hat{S}_l$.

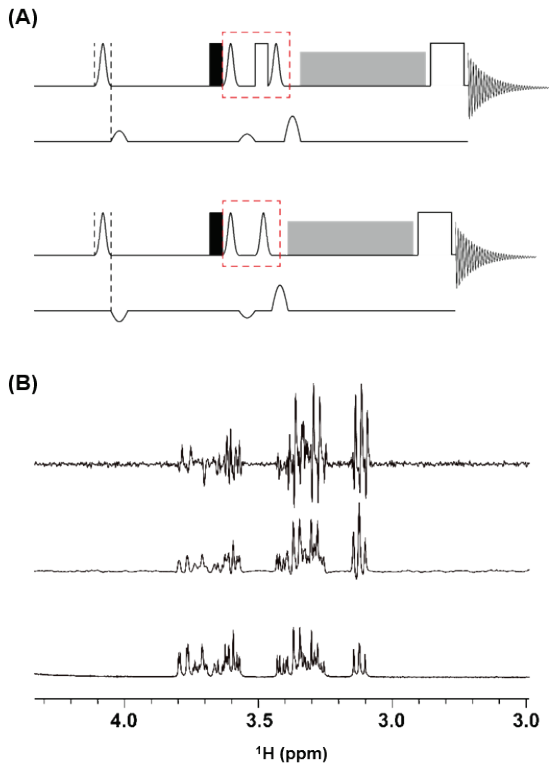

Figure 2. (A) Comparison of modified (upper) and original (lower) iSQC with the adiabatic spinlock (asl). Dashed-boxes are indicate differences between modified and original iSQC sequences with asl. **(B)** Stacked 1D projection spectra of original (upper)/ modified (middle) iSQC spectra and ^{1}H NMR spectrum (lower) of D-glucose.

Because the shape of the first-kind Bessel function is similar to attenuating sinusoidal function, it was usually required a certain delay time, Δ, before an amplitude of iSQC signal reaches its apex. As stated, intramolecular J-coupling during the Δ can give rise to J-modulated NMR signal. Fugariu *et al.*[11] introduced an adiabatic mixing pulse sequence[13] into this type of experiment instead of simple spin-echo pulse sequence. Although, by the consequence of isotropic mixing sequence[14], a certain ratio of magnetizations will be transferred to another J-coupled spins, we can retain an in-phase magnetization during the spinlock period with an avoiding the J-modulation of signal. Moreover, an adiabatic inversion is quite insensitive to spatial inhomogeneity in B_1 or B_0,[15] thus it is more suitable for inhomogeneous sample which has non-zero field inhomogeneity ($B\Delta(z)$).

Results and Discussion

When we tested, however, the in-phase iSQC sequence suggested by Fugariu *et al.*[11] a chemical shift dependent phase accumulation was appeared. This type of accumulation was turned out that it is due to a chemical shift evolution during the second and third gradient pulse pair. To address this, we inserted a spin-echo inversion pulse between two gradient pair. Figure 2A shows comparison of iSQC spectra with/without the inversion pulse between gradient pair. We tested the modified iSQC sequence using D-glucose sample. Figure 2B shows the comparison of the 1D projection spectra of the 2D spectra produced by each iSQC pulse sequence and the conventional ^{1}H spectrum. Without the spin-echo inversion (Figure 2B, upper), a chemical shift dependent phase accumulation was exhibited, whereas, with insertion of spin-echo inversion (Figure 2B middle), a desirable in-phase signal was obtained.

According to DDF theory[12], the valid distance of dipolar coupling between two spins in liquid state is can be defined as a correlation distance; $d_c = \frac{\pi}{\gamma G \delta}$. Thus, in case of typical NMR spectrometers, the correlation distance is within hundreds of micrometers. Faber et al.[5, 10] reported some papers which exploit this DDF effect for a separation between intra and extra cellular NMR signals using NMR phantom and oocytes by an adjusting the correlation distance smaller than internal diameters of phantom or oocytes. We can exploit similar principle for the sample in which consists of two or more immiscible liquid phases. As stated, a locally induced DDF can only effect small amount of ranges ($\sim d_c$). Thus, in a physically separated two liquid system, we can acquire selective solute NMR signals dissolved in a specific solvent by applying a selective excitation pulse for the specific solvent signal.

As a model system, we chose a two-phase liquid system; D-glucose in water/ palmitic acid in chloroform. A pictorial illustration and real picture of a two-phase liquid NMR sample is shown in Figure 1B. Since water and chloroform are immiscible solvent, an interface between two solvents appeared in Figure 1B. In addition, the carbohydrate is not soluble in chloroform and the fatty acid is also not soluble in water, thus each solute can only exist on own soluble solvent. The difference in chemical shift between water and chloroform is large enough to selectively excite by a shaped pulse with a practical duration ranges. If the difference in chemical shift between solvent is too small, then using a paramagnetic shift reagent[16] will be aid of resulting in a sufficient separation of resonance frequencies. In each iSQC NMR acquisitions, by switching the offset frequency of the shaped pulse to the resonance frequency of specific solvent, individual solute NMR spectra were acquired respectively. Figure 3A and 3B are 2D iSQC spectra of water and chloroform phase respectively. In figure 3C, 1D projection spectra along the F_2 domain (Figure 3C, upper and middle) and conventional ^{1}H NMR mixture spectrum (Figure 3C, lower) were exhibited. In the conventional NMR spectrum, the whole solute NMR signals in each two liquid phases were acquired, whereas each projection spectra only showed specific individual NMR signals according to the selection shaped pulse respectively. Before the acquisition start, in order to suppress residual water signal, WATERGATE (W5) by double echo gradients[17] was inserted. In the figure 3C (upper), signal attenuation of anomeric protons (α- and β-) and protons near the 4 ppm on account of suppression of W5 sequence was exhibited. For acquisition of chloroform phase, large residual water signal (another phase) was appeared. Additional solvent suppression or pre-saturation sequence for the water resonance may alleviate generation of residual signal. Although we used same molar concentration for each solute (100 mM), it seems the chloroform phase signal shows much lower signal-to-noise ratio compare to water phase signal. As we used single adiabatic mixing sequence duration value (80 ms) for each parallel iSQC acquisition, it is believed a different solvent environment might affect the signal amplitude curve $J_1\left(\frac{2}{3}\tau_{dI}^{-1}t_2'\right)$ of DDF effect.

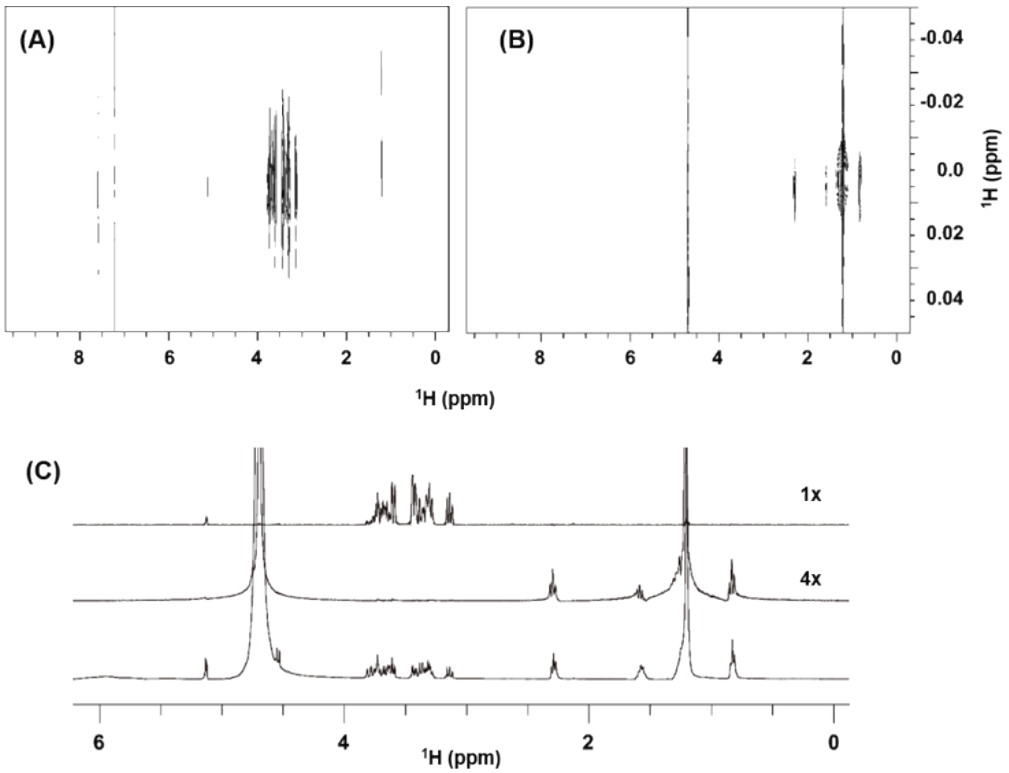

Figure 3. Results of modified iSQC spectra with adiabatic spinlock for the two-phase liquid system; Sample system consist of D-glucose in water/ palmitic acid in chloroform (each 100 mM). **(A)** 2D iSQC spectrum of the water phase; An offset frequency of gaussian shaped pulses was set to the resonance frequency of the water signal. **(B)** 2D iSQC spectrum of the chloroform phase; An offset frequency of gaussian shaped pulses was set to the resonance frequency of the chloroform signal. **(C)** Stacked 1D projection spectra from (A, upper), (B, middle) and conventional ^{1}H NMR spectrum (lower) of sample.

Conclusions

Here, we showed that solvent-localized NMR signals can be acquired from two immiscible solvents system through the iSQC based experiment. A simple modification of the previous iSQC sequence gives accurate in-phase iSQC signal. By using the modified iSQC sequence and switching the offset frequency of selective pulse, we acquired solvent specific solute NMR signals. In general, NMR shiming process in two different liquid system is considered to harder than a typical homogenious single liquid system. On the contrary, the iSQC signal is immune to modrate field inhomogeneity[8], thereby can give homogenous NMR signal. We believe our approaches might be useful in metabolic analysis using such as two-phase liquid extraction scheme for some labile chemical species.

Experimental section

General NMR measurements- All NMR spectra were measured at 298 K with 400 MHz Bruker Avance III HD spectrometer equipped with 5 mm BBO Probe (Bruker BioSpin, Germany). For the preparation of two phase liquid NMR sample, D-glucose (100 mM, Sigma-Aldrich, MO, USA) and pamitic acid (100 mM, Sigma-Aldrich, MO, USA) were dissolved in 300 μL of water (Sigma –Aldrich, MO, USA) and 300 μL of chloroform (DUKSAN, Korea), respectively. For the magnetic field lock, water contains 20% of deuterium oxide (Cambridge isotope, MA, USA).

iSQC sequence- For the acquisition of the iSQC sequence, the interscan delay was set to 3 s and the number of transient was 16. The duration of the adiabatic

mixting pulse was 80 ms and the acquisition time was 400 ms. Spectral width was 10 ppm, carrier frequency of the F_2 domain was set to 4.68 and the F_1 domain was set to, according to solvent resonance, 4.68 and 7.16 ppm, respectively. The ratio of *z*-gradent pulses in sequence was set at 0.7 : 1 : 2.4, in the order and their duration δ was set to 1 ms. A gradient recovery delay was 100 μs. A correlation distance $d_c = \frac{\pi}{\gamma G \delta}$ was set to *ca.* 230 μm.

Adiabatic mixing pulse sequence- Generation and calibration of the adiabatic inversion pulse were carried out using a shapetool™ from Tospin 3.61. Waveform = Constant adiabaticicy(ca.)-WURST-2. Sweep width = 16 kHz. Pulse duration: 320 μs. $\gamma B_{1,max}$ = 6512 Hz. MLEV-16 TOCSY supercycle was employed.

Solvent suppression- For the solvent signal suppression, WATERGATE(W5) with double echo gradients was employed. The delay for the binomial suppression was set to 125 μs.

Solvent selective pulse- For the solvent selective shaped pulse Gaussian pulse with 4.24 ms duration was employed. Offset frequency of Gaussian pulse was adjusted to each solvent resonance frequency.

Data Processing- For 2D iSQC spectrum, the actual time-domain porints were 3198×18 (t_2×t_1) points wih the final 8192×2048 points (F_2×F_1) after forward and backward linear prediction[18] and zero-filling processing. Each 1D projection spectra were obtained by F_2 projection of 2D iSQC spectra after proper spectrum rotation processing.

Appendix

The expression for the equilibrium density matrix consist of two spin (**I** and **S**) without the high-temperature approximation[2] can be expressed as

$$\hat{\sigma}_{eq} \propto \mathbf{1} + \sum_i \sum_j \hat{I}_{iz}\hat{S}_{jz} + \text{high-order terms} \qquad \textbf{(16)}$$

where, the indices i and j are increased up to the number of **I** and **S** spins, respectively.

Here, for brevity, we only consider two-spin density matrix terms.
The coherence transfer pathway which is valid in the suggested pulse sequence (Figure 1) is,

$$0 \;\rightarrow\; +1 \;\rightarrow\; +2 \;\rightarrow\; -1$$

Thereby, the observable density operator description via the pulse sequence is shown as follows

$$\begin{aligned}
&\sum_i \sum_j \hat{I}_{iz}\hat{S}_{jz} \xrightarrow{(\pi/2)_x^I} \xrightarrow{\gamma G z \delta} \xrightarrow{\Omega_I \hat{I}_z t_1} \\
&\sum_i \sum_j \hat{I}_{i+}\hat{S}_{jz} \exp(-i\Omega_I t_1) \exp(-i\gamma G z_i \delta) \\
&\qquad \times \exp(-i\gamma \Delta B(z_i) t_1) \xrightarrow{(\pi/2)_x^{I+S}} \xrightarrow{(-\pi/2)_x^I} \xrightarrow{\gamma 0.7 G z \delta} \\
&\sum_i \sum_j \hat{I}_{i+}\hat{S}_{j+} \exp(-i\Omega_I t_1) \exp(-1.7 i\gamma G z_i \delta) \\
&\qquad \times \exp(-0.7 i\gamma G z_j \delta) \exp(-i\gamma \Delta B(z_i) t_1) \\
&\qquad\qquad \xrightarrow{\pi_x^{I+S}} \xrightarrow{(\pi/2)_x^I} \xrightarrow{\gamma 2.4 G z \delta} \\
&\sum_i \sum_j \hat{I}_{iz}\hat{S}_{j-} \exp(-i\Omega_I t_1) \exp\left(-i1.7\gamma G(z_i - z_j)\delta\right) \\
&\qquad \times \exp(-i\gamma \Delta B(z_i) t_1) \\
&\qquad\qquad \xrightarrow{\hat{\mathscr{H}}_{DD}(\Delta + t_2)} \xrightarrow{\Omega_S \hat{S}_z (\Delta + t_2)} \\
&\qquad i\frac{1}{2}\hat{S}_- \exp(-i\Omega_I t_1) \exp(-i\gamma \Delta B(z) t_1) \\
&\qquad\qquad \times \exp(i\Omega_S t_2) \exp(i\gamma \Delta B(z) t_2)\, A\left(t_2'\right)
\end{aligned} \qquad \textbf{(17)}$$

$$\xrightarrow{I\text{-}S\,\mathrm{DD\ interaction}} \overset{*\ \hat{I}_z\hat{S}_-}{\hat{I}_z\hat{S}_- \cos\left\{\frac{3}{2}D_{ij}(\Delta + t_2)\right\}} + i\frac{1}{2}\ \hat{S}_- \sin\left\{\frac{3}{2}D_{ij}(\Delta + t_2)\right\}$$

where, $\hat{\mathscr{H}}_{DD} = \sum_i \sum_j 3D_{ij}^{IS}\, \hat{I}_{iz}\hat{S}_{jz}$, and $D_{ij}^{IS} = \frac{\mu_0}{4\pi} \cdot \frac{\gamma_I \gamma_S \hbar}{4} \cdot \frac{1 - 3\cos^2\theta_{ij}}{r_{ij}^3}$. r_{ij} is the distance between spins i and j, θ_{ij} is the angle between the inter nuclear vector and magnetic field, B_0, and $A\left(t_2';\ \Delta + t_2\right)$ is the amplitude function.

Thereby, we can get the similar density matrix form in **(17)** as the equation **(13)**.

Acknowledgements

This work was supported by the Korea Institute of Science & Technology—Research Program (2Z06220).

References

1. S. Lee, W. Richter, S. Vathyam and W. S. Warren, *J. Chem. Phys.* **105**, 3 (1996)
2. S. Ahn, W. S. Warren and S. Lee, *J. Magn. Reson.* **128**, 2 (1997)
3. S. Ahn, N. Lisitza and W. S. Warren, *J. Magn. Reson.* **133**, 2 (1998)
4. W. S. Warren, W. Richter, A. H. Andreotti and B. T. Farmer, *Science* **262**, 5142 (1993)
5. C. Faber, *J. Magn. Reson.* **176**, 1 (2005)
6. S. Vathyam, S. Lee and W. S. Warren, *Science* **272**, 5258 (1996)
7. Q. H. He, W. Richter, S. Vathyam and W. S. Warren, *J. Chem. Phys.* **98**, 9 (1993)
8. Y. Q. Huang, S. H. Cai, X. Chen and Z. Chen, *J. Magn. Reson.* **203**, 1 (2010)
9. Z. Chen, Z. W. Chen and J. H. Zhong, *J. Am. Chem. Soc.* **126**, 2 (2004)
10. V. Hoerr, A. Purea and C. Faber, *Biophys. J.* **99**, 7 (2010)
11. I. Fugariu, W. Bermel, D. Lane, R. Soong and A. J. Simpson, *Angew. Chem. Int. Ed.* **56**, 22 (2017)
12. D. Z. Balla and C. Faber, *Concepts Magn. Reson. A* **32a**, 2 (2008)
13. W. Peti, C. Griesinger and W. Bermel, *J. Biomol. NMR* **18**, 3 (2000)
14. L. Braunschweiler and R. R. Ernst, *J. Magn. Reson.* **53**, 3 (1983)
15. R. A. DeGraaf and K. Nicolay, *Concepts Magn. Reson.* **9**, 4 (1997)
16. R. V. Ammon and R. D. Fischer, *Angew. Chem. Int. Ed.* **11**, 8 (1972)
17. M. L. Liu, X. A. Mao, C. H. Ye, H. Huang, J. K. Nicholson and J. C. Lindon, *J. Magn. Reson.* **132**, 1 (1998)
18. P. Sakhaii and W. Bermel, *J. Magn. Reson.* **242**, (2014)